



Modeling atmospheric sulfate oxidation chemistry via the oxygen isotope mass-independent fractionation using the Community Multiscale Air Quality Model (CMAQ)

Huan Fang¹, Wendell Walters¹

¹Department of Chemistry and Biochemistry, University of South Carolina, SC, 631 Sumter Street Columbia, SC 29208, United States

Correspondence to: Wendell Walters (wendellw@mailbox.sc.edu)

Abstract. Atmospheric sulfate formation influences climate and air quality, yet its chemical pathways remain difficult to constrain. This study utilizes the oxygen isotope anomaly ($\Delta^{17}\text{O}$) of sulfate aerosol (ASO_4) as a tracer to distinguish formation processes. For the first time, we modeled $\Delta^{17}\text{O}(\text{ASO}_4)$ using the Community Multiscale Air Quality Model (CMAQ), focusing on 2006 and 2019 to quantify key ASO_4 formation pathways and their response to U.S. emission changes. In 2006, $\Delta^{17}\text{O}(\text{ASO}_4)$ values were predicted to be below 1‰ in the Gulf Coast indicated acidic, ASO_4 -rich conditions dominated by $\text{S(IV)} + \text{H}_2\text{O}_2$ oxidation, while values above 1‰ in the West suggested less acidic conditions, leading to enhanced ASO_4 production via $\text{S(IV)} + \text{O}_3$ oxidation. Peak $\Delta^{17}\text{O}(\text{ASO}_4)$ values of ~5‰ in April across the Western U.S. reflected O_3 -driven ASO_4 formation during high ammonia (NH_3) emissions from fertilization. Between 2006 and 2019, mean $\Delta^{17}\text{O}(\text{ASO}_4)$ increased by up to 2‰, driven by declining sulfur dioxide (SO_2) emissions from regulatory measures. Model comparisons with historical measurements show reasonable agreement in the acidic southeastern U.S. (RMSE = 0.3‰, Baton Rouge, LA). However, the model overpredicts $\Delta^{17}\text{O}(\text{ASO}_4)$ in the West, with RMSE values of 0.5‰ (La Jolla, CA) and 2.1‰ (White Mountain Research Center, CA), particularly during periods of high NH_3 emissions. This overestimation suggests an excessive model response to aqueous $\text{S(IV)} + \text{O}_3$ reactions. These results emphasize the need for expanded $\Delta^{17}\text{O}(\text{ASO}_4)$ measurements and improved model constraints to better capture evolving emission trends and regulatory impacts on sulfate formation.

1 Introduction

Atmospheric sulfate (SO_4^{2-}) plays a critical role in climate and air quality. As a major component of aerosols, SO_4^{2-} influences aerosol pH, atmospheric chemistry, and precipitation acidity (Calvo et al., 2013; Weber et al., 2016). SO_4^{2-} aerosols (ASO_4) significantly contribute to radiative forcing by scattering sunlight and serving as cloud condensation nuclei, which impacts cloud properties and the Earth's radiation balance (Lohmann & Feichter, 1997; Jones et al., 1994; Kaufman & Tanré, 1994). The anthropogenic influence on the ASO_4 budget, primarily from fossil fuel combustion, has been widely



30 documented, contributing to regional and global climate effects (Langner et al., 1992; Smith et al., 2011). The presence of
ASO₄ alters cloud albedo and lifetime, affecting regional and global climate patterns through indirect radiative forcing (Jones
et al., 1994; Haywood & Boucher, 2000). Additionally, the health impacts of ASO₄-containing particles underscore their
importance in air quality management (Reiss et al., 2007). The formation of ASO₄ is influenced by complex interactions with
secondary organic aerosols (SOA) and other atmospheric components, with emerging research highlighting the significant
35 role of highly oxygenated organic molecules (HOMs) in enhancing ASO₄ formation under humid conditions (Hallquist et al.,
2009; Bianchi et al., 2019). These interactions highlight the complex connections between ASO₄, atmospheric chemistry,
and climate dynamics. Despite a 70% reduction in sulfate concentrations over the past 15 years, aerosol acidity has remained
high, largely driven by the buffering effect of ammonia partitioning between gas and particle phases (Weber et al., 2016).
This persistent acidity impacts both air quality and health, as it enhances the solubility of harmful metals and promotes acid-
40 catalyzed chemical reactions in the atmosphere.

Despite their significance, atmospheric chemistry models often face significant challenges in accurately reproducing ASO₄
concentrations, potentially due to uncertainties surrounding ASO₄ formation mechanisms (Harris et al., 2013; Li et al., 2020;
Vannucci et al., 2024). ASO₄ can originate from both primary emissions and secondary formation. Primary sources include
45 natural emissions, such as sea salt, volcanic eruption, and soil dust (Alexander et al., 2005; Arimoto et al., 2001; Savarino et
al., 2003), as well as anthropogenic emissions from fossil fuel combustion (Langner et al., 1992; Smith et al., 2011; Solfen et
al., 2011). Secondary ASO₄ formation involves complex oxidation processes, occurring in both the gas phase and aqueous
phase. In the gas phase, sulfur dioxide (SO₂) is oxidized by hydroxyl radicals (OH), producing sulfuric acid (H₂SO₄). This
sulfuric acid can either condense to form new particles or add mass to existing aerosols. The rate of this process is highly
50 dependent on environmental conditions such as temperature and pH, which introduces significant uncertainties in predicting
ASO₄ concentrations (Seigneur & Saxena, 1988). For instance, Vannucci et al. (2024) demonstrated that temperature plays a
critical role in modulating sulfate aerosol concentrations, particularly during summertime pollution episodes, where aerosol
composition and temperature sensitivity can strongly influence model accuracy. Aqueous-phase ASO₄ formation occurs
when dissolved sulfur species (S(IV) = SO₂·H₂O + HSO₃⁻ + SO₃²⁻) are oxidized by molecules including ozone (O₃),
55 hydrogen peroxide (H₂O₂), and oxygen catalyzed by transition metal ions (TMI) (e.g., Fe³⁺ and Mn²⁺). Sensitivity analyses
have shown that the rate of aqueous-phase ASO₄ formation is particularly influenced by pH, oxidant availability, and
environmental conditions, further complicating ASO₄ modeling (Pandis & Seinfeld, 1989). Harris et al. (2013) showed that
TMI-catalyzed oxidation can dominate under specific conditions, particularly in the presence of coarse dust particles,
significantly altering sulfate formation rates in cloud droplets. Similarly, Li et al. (2020) highlighted the critical role of TMI-
60 driven SO₂ oxidation during haze episodes, where such pathways can account for up to 50% of sulfate production under
polluted conditions. Heterogeneous reactions on aerosol surfaces may also play a critical role in ASO₄ formation (Harris et
al., 2013). These surface reactions involve the interaction of gaseous sulfur species with aerosols, significantly influencing
ASO₄ formation and elevating the complexity of predicting ASO₄ concentrations. Meidan et al. (2019) emphasized the



importance of Criegee intermediates (CIs) in sulfate formation, particularly in nocturnal power plant plumes, where SO₂ is
65 oxidized under conditions with minimal photochemical activity. This study revealed that CIs could account for a significant
portion of sulfate aerosol production in the absence of sunlight. Additionally, Liu et al. (2019) examined the role of
stabilized Criegee intermediates (sCIs) in sulfate formation in the Beijing-Tianjin-Hebei region, showing that under certain
atmospheric conditions, sCI-driven SO₂ oxidation can contribute substantially to secondary sulfate production, adding
another layer of complexity to sulfate formation models. These interactions underscore the challenges in modeling ASO₄
70 concentrations, with heterogeneous reactions, TMIs, and Criegee intermediates all contributing to the uncertainty in
atmospheric sulfate predictions.

The use of oxygen isotope mass-independent fractionation ($\Delta^{17}\text{O} = \delta^{17}\text{O} - 0.52 \times \delta^{18}\text{O}$) has emerged as a promising tool to
explore atmospheric ASO₄ formation pathways (Alexander et al., 2004; Barkan & Luz, 2003; Kaiser et al., 2004; Michalski
75 et al., 2003; Morin et al., 2007; Savarino et al., 2007; Walters et al., 2019; Weston, 2006). This isotopic indicator is crucial
for tracking ASO₄ formation, providing a refined tool for model evaluation and prediction. This is because $\Delta^{17}\text{O}$ has distinct
values associated with different oxidation processes, making it a powerful tool in understanding ASO₄ production
mechanisms. The dominant source of $\Delta^{17}\text{O}$ in the lower atmosphere derives from O₃ formation. The average $\Delta^{17}\text{O}(\text{O}_3)$ near
the surface is approximately 26‰ (Vicars & Savarino, 2014). This contrasts with other tropospheric oxidants, which have
80 $\Delta^{17}\text{O}$ values near 0‰. For example, hydrogen peroxide (H₂O₂) has a $\Delta^{17}\text{O}$ value of about 1.6‰ due to influences of O₃
involved in H₂O₂ formation (Savarino & Thiemens, 1999). Laboratory studies show that aqueous-phase oxidation by both
H₂O₂ and O₃ proportionally transfers their $\Delta^{17}\text{O}$ values to ASO₄ (Savarino et al., 2000). The role of other oxidants, such as
hypohalous acids (HOX, X = Cl and Br), is increasingly recognized, particularly in marine boundary layers (Chen et al.,
2016; Ishino et al., 2017). Chen et al. (2016) highlighted the significant contribution of HOX in sulfate formation in the
85 remote marine boundary layer, estimating that 33-50% of sulfate is produced via this pathway. This suggests that HOX may
play a larger role in sulfate aerosol formation than previously recognized, potentially altering $\Delta^{17}\text{O}$ values associated with
ASO₄ production. Recent studies also highlight the impact of anthropogenic emissions on ASO₄ production routes. In
polluted regions, anthropogenic emissions of metals such as Fe and Mn enhance O₂-catalyzed ASO₄ formation, particularly
in the Northern Hemisphere during winter. This metal-catalyzed ASO₄ formation can suppress ASO₄ production via O₃ and
90 H₂O₂ pathways, impacting $\Delta^{17}\text{O}(\text{ASO}_4)$ values and complicating model predictions (Savarino et al., 2000). Furthermore, ship
emissions, which have been underrepresented in atmospheric models, significantly contribute to ASO₄ source in marine
environments. Triple-oxygen isotope measurements suggest these emissions play a larger role in ASO₄ production than
previously recognized, with implications for air quality and climate modeling (Dominguez et al., 2008).

Table 1 summarizes the $\Delta^{17}\text{O}$ ranges associated with major tropospheric non-sea-salt ASO₄ production pathways based on
95 oxygen isotopic mass balance (Alexander et al., 2005; Alexander et al., 2009; Ishino et al., 2017; Savarino et al., 2000;
Walters et al., 2019). Gas-phase oxidation of SO₂ by OH and metal-catalyzed O₂ oxidation yields $\Delta^{17}\text{O}(\text{ASO}_4)$ values near
0‰, indicating negligible mass-independent fractionation. Similarly, aqueous-phase oxidation of SO₂ by hypohalous acids



(HOX) results in $\Delta^{17}\text{O}$ values around 0‰. In contrast, aqueous-phase oxidation involving H_2O_2 and O_3 exhibits significantly higher $\Delta^{17}\text{O}$ values. H_2O_2 oxidation produces $\Delta^{17}\text{O}$ values around 0.8‰, while O_3 oxidation results in $\Delta^{17}\text{O}$ values of about 6.5‰. These distinctions enable the ability to track ASO_4 formation.

Table 1: Major ASO_4 formation pathways and their associated $\Delta^{17}\text{O}$ signatures. The pathways that are included in the CMAQ model using the cb6r5-ae7-aq mechanism are indicated.

Pathway	Reaction	$\Delta^{17}\text{O}$ (‰)	Notes	Included in CMAQ (cb6r5-ae7)
Gas-Phase	$\text{SO}_2 + \text{OH} \rightarrow \text{SO}_4^{2-} + \text{HO}_2$	~0	Dominant in photochemically active regions; negligible $\Delta^{17}\text{O}$ signature	No
Aqueous-Phase	$\text{HSO}_3^- + \text{H}_2\text{O}_2 \rightarrow \text{SO}_4^{2-} + \text{H}_2\text{O}$	0.8	Lower $\Delta^{17}\text{O}$ value, dominant under humid/cloudy conditions.	Yes
Aqueous-Phase	$\text{SO}_3^{2-} + \text{O}_3 \rightarrow \text{SO}_4^{2-} + \text{O}_2$	6.5	Higher $\Delta^{17}\text{O}$ value, significant for cloud chemistry.	Yes
Aqueous-Phase	$\text{SO}_3^{2-} + \text{O}_2$ (TMI = Transition Metal Ions, e.g., Fe^{3+} and Mn^{2+}) $\rightarrow \text{SO}_4^{2-}$	~0	Important in metal-rich aerosols; negligible $\Delta^{17}\text{O}$ signature	No
Aqueous-Phase	$\text{SO}_3^{2-} + \text{HOX}$ (X = Br, Cl) $\rightarrow \text{SO}_4^{2-}$	~0	Dominant in marine environments with halogen chemistry; negligible $\Delta^{17}\text{O}$ signature	No
Heterogeneous	SO_2 (surface) + Organic peroxides $\rightarrow \text{SO}_4^{2-}$	~0	Significant role in submicron aerosol sulfate formation; negligible $\Delta^{17}\text{O}$ signature.	No
Heterogeneous	SO_2 (surface) + H_2O_2 or O_3 on aerosols $\rightarrow \text{SO}_4^{2-}$	0.8 - 6.5	Highly variable; depends on aerosol composition and environmental conditions.	No

To fully utilize the diagnostic potential of $\Delta^{17}\text{O}(\text{ASO}_4)$, a comprehensive model framework for interpreting ASO_4 formation is essential. Previous models, such as GEOS-Chem, have incorporated $\Delta^{17}\text{O}$ tracking to investigate sulfate formation pathways, highlighting the growing importance of metal-catalyzed O_2 oxidation in polluted regions, which surpasses the traditional O_3 and H_2O_2 pathways (Sofen et al., 2011). Despite rising tropospheric O_3 levels since preindustrial times,



$\Delta^{17}\text{O}(\text{ASO}_4)$ values in the Arctic have declined due to enhanced metal-catalyzed sulfate formation. Still, there are motivation
110 to add the ability to model $\Delta^{17}\text{O}$ using other model frameworks, particularly for models relevant for air quality, deposition,
and policy. In this work, $\Delta^{17}\text{O}$ tracking has now been incorporated into the Community Multiscale Air Quality Model
(CMAQ), a 3-D atmospheric chemistry transport model. CMAQ offers high spatial and temporal resolution, which is critical
for studying ASO_4 formation pathways and for validating model predictions through observational testing (Appel et al.,
2021). This study aims to refine ASO_4 formation modeling by integrating $\Delta^{17}\text{O}$ tracking into CMAQ, thus improving
115 predictions of ASO_4 dynamics and reducing uncertainties in atmospheric chemistry models. The spatiotemporal $\Delta^{17}\text{O}$ values
predicted by CMAQ will help validate model predictions and advance our understanding of atmospheric ASO_4 chemistry
and its connection to air quality and deposition. Establishing reference $\Delta^{17}\text{O}$ values across the contiguous United States
(CONUS) is a key outcome of this study, as it lays the groundwork for future research, enhances air quality and deposition-
related studies, and contributes to improved air quality management strategies by providing a more accurate representation
120 of sulfate formation across different regions.

2 Methods

2.1 Model Description and EQUATES 2019 Dataset

This study utilizes the CMAQ (Community Multiscale Air Quality) version 5.4 model to simulate ASO_4 formation and its
 $\Delta^{17}\text{O}$ values across the contiguous United States (CONUS). The CMAQ model is configured with the cb6r5_ae7_aq
125 chemical mechanism, which stands for Carbon Bond 6 revision 5, with aerosol 7 for standard cloud chemistry (Yarwood et
al., 2010). This mechanism includes both gas-phase and aqueous-phase oxidation processes of SO_2 , essential for accurately
modeling ASO_4 formation. Specifically, it involves the oxidation of SO_2 by OH in the gas phase and by H_2O_2 and O_3 in
cloud droplets and aqueous environments. The model's ability to capture these complex interactions facilitates a detailed
assessment of ASO_4 dynamics under various atmospheric conditions (Appel et al., 2021).

130 The CMAQ simulations are based on the EQUATES (EPA's Air Quality Time Series Project) dataset, which provides a
comprehensive and high-resolution emissions inventory derived from the 2017 National Emissions Inventory (NEI) (Benish
et al., 2022; Foley et al., 2023). This dataset covers over two decades and includes detailed information on both natural and
anthropogenic emissions, such as those from industrial sources, vehicular traffic, power plants, and wildfires. It also
135 accounts for seasonal and regional variations in emissions, enhancing the model's accuracy. The EQUATES 2019 dataset
supplies critical inputs for CMAQ simulations, including emissions data, meteorological variables, as well as boundary and
initial conditions, capturing pollutant variability across different seasons and regions.

Meteorological inputs for the CMAQ simulations were integrated from the Weather Research and Forecasting (WRF) model
140 version 4.1.1. This integration provides detailed representations of temperature, wind speed, relative humidity, cloud cover,



and precipitation rates. These meteorological factors influence cloud formation, pollutant dispersion, and oxidation processes. Boundary and initial conditions for the CMAQ model were sourced from EQUATES to ensure accurate representation of pollutant inflows and outflows at the edges of the modeling domain. The initial conditions were established through a spin-up period starting on December 15, 2018, providing accurate starting concentrations for the 2019 simulation period. The CMAQ simulations were conducted at a resolution of 12×12 km over the CONUS domain using the Hyperion high-performance computing cluster at the University of South Carolina. This advanced computing infrastructure enabled the processing of large datasets and the execution of complex simulations necessary for this study.

2.2 Implementation of the Sulfur Tracking Mechanism (STM)

The Sulfur Tracking Mechanism (STM), utilized in the CMAQ model, provides a detailed analysis of ASO_4 formation pathways in the atmosphere (Appel et al., 2021). It distinguishes between various aqueous-phase and gas-phase formation processes and assesses contributions from emissions, initial conditions, and boundary conditions, offering valuable insights into the roles of these factors in overall ASO_4 production (Table 2). The sulfur budget includes 14 ASO_4 species (AE) and 1 nonreactive ASO_4 species (NR), as documented in the CMAQ repository: (<https://github.com/USEPA/CMAQ/blob/main/CCTM/src/MECHS/README.md>.) The STM output includes hourly simulations of the 15 tagged ASO_4 species across the model domain, which were then aggregated into monthly averages to analyze spatial and temporal variations in ASO_4 production. STM allows for an efficient way for the model to distinguish the contributions of different chemical pathways and emission contributions to ASO_4 . This approach also enables for a seamless calculation of $\Delta^{17}\text{O}$ of ASO_4 .

Table 2: Overview of the sulfate species in the Sulfur Tracking Mechanism (STM) incorporated into CMAQ.

Name	Group	Mode	Pathway
ASO4GASI	AE	Aitken	condensation of gas-phase reaction with OH
ASO4EMISI	AE	Aitken	source emission
ASO4ICBCI	AE	Aitken	initial conditions and boundary conditions
ASO4AQH2O2J	AE	Accumulation	H_2O_2
ASO4AQO3J	AE	Accumulation	O_3
ASO4AQFEMNJ	AE	Accumulation	O_2 catalyzed by Fe^{3+} and Mn^{2+}
ASO4AQMHPJ	AE	Accumulation	methyl hydrogen peroxide (MHP)
ASO4AQPAAJ	AE	Accumulation	peroxyacetic acid (PAA)
ASO4GASJ	AE	Accumulation	condensation of gas-phase reaction with OH
ASO4EMISJ	AE	Accumulation	source emission



ASO4ICBCJ	AE	Accumulation	initial conditions and boundary conditions
ASO4GASK	AE	Coarse	condensation of gas-phase reaction with OH
ASO4EMISK	AE	Coarse	source emission
ASO4ICBCK	AE	Coarse	initial conditions and boundary conditions
SULF_ICBC	NR	N/A	sulfuric acid vapor (SULF) from initial conditions and boundary conditions

2.3 Calculation and Analysis of $\Delta^{17}\text{O}(\text{ASO}_4)$

The fractional contributions of each pathway, obtained from the STM, are used to calculate $\Delta^{17}\text{O}(\text{ASO}_4)$ across different grid cells.

$$f_i(\text{lat}, \text{lon}, \text{height}, \text{time}) = \frac{x_i}{\sum_{i=1}^n x_i} \quad (1)$$

where f_i represents the fractional contribution of pathway i ; x_i is the amount of ASO_4 produced by pathway i ; and $\sum_{i=1}^n x_i$ is the total Aitken mode and accumulation mode ASO_4 produced by all pathways except initial conditions and boundary conditions in each grid cell.

The gas-phase oxidation of SO_2 by OH radical results in ASO_4 with no significant $\Delta^{17}\text{O}$ enrichment ($\sim 0\text{‰}$). ASO_4 formed via aqueous-phase oxidation by O_3 has a $\Delta^{17}\text{O}$ value of $\sim 6.5\text{‰}$, indicating significant cloud chemistry processes. ASO_4 formed via aqueous-phase oxidation by H_2O_2 has a $\Delta^{17}\text{O}$ value of $\sim 0.8\text{‰}$. Metal-catalyzed oxidation of SO_2 by O_2 in metal-rich environments results in $\Delta^{17}\text{O} \sim 0\text{‰}$ and does not show mass-independent fractionation. Heterogeneous reactions, such as those involving organic peroxides on aerosol surfaces, contribute to ASO_4 formation and are expected to have a $\Delta^{17}\text{O} \sim 0\text{‰}$. Among these oxidation pathways, only H_2O_2 and O_3 are dominant and lead to ASO_4 with a non-zero $\Delta^{17}\text{O}$. Therefore, the $\Delta^{17}\text{O}(\text{ASO}_4)$ is calculated using the following equation:

$$\Delta^{17}\text{O}(\text{ASO}_4) = f_{\text{ASO4AQH2O2J}} \times 0.8\text{‰} + f_{\text{ASO4AQO3J}} \times 6.5\text{‰} \quad (2)$$

where ASO4AQH2O2J represents ASO_4 formed through the oxidation of SO_2 by H_2O_2 ; ASO4AQO3J represents ASO_4 formed through oxidation by O_3 ; the constants 0.8‰ and 6.5‰ correspond to the characteristic $\Delta^{17}\text{O}$ values for each pathway.

3 Results and Discussion

3.1 Predicted Fractional ASO_4 Formation and $\Delta^{17}\text{O}(\text{ASO}_4)$ in the Contiguous US in 2019

ASO_4 production in the contiguous United States arises from a combination of primary emissions and secondary formation pathways, the latter being dominated by aqueous-phase reactions (Fig. 1). These secondary reactions occur within cloud



185 water, where SO_2 is oxidized by H_2O_2 , O_3 , or TMI (Fe^{3+} and Mn^{2+}). Additionally, organic peroxides such as methyl hydrogen peroxide (MHP) and peroxyacetic acid (PAA), as well as the gas-phase oxidation of SO_2 by OH were predicted to have a minimal impact on ASO_4 production in the US.

The fractional contributions of ASO_4 formation pathways demonstrate distinct spatial patterns that align with the predicted
190 $\Delta^{17}\text{O}(\text{ASO}_4)$ variability. The H_2O_2 pathway ($f_{\text{S(IV)}+\text{H}_2\text{O}_2}$) is the most dominant, accounting for 48.5% of the sulfate formation across the domain (Fig. 1). This pathway is particularly influential in the Gulf Coast States, where abundant cloud cover and water vapor, acidic conditions (cloud $\text{pH} < 6$), and high concentrations of H_2O_2 (Fig. S1, Fig. S2) support the oxidation of S(IV) in cloud droplets. The highest $f_{\text{S(IV)}+\text{H}_2\text{O}_2}$ in these regions contribute to the low $\Delta^{17}\text{O}(\text{ASO}_4)$ values below 2‰, due to the relatively lighter $\Delta^{17}\text{O}(\text{ASO}_4)$ resulted from the H_2O_2 pathway (0.8‰). The O_3 pathway ($f_{\text{S(IV)}+\text{O}_3}$) is the
195 second most significant, contributing approximately 26.3% to the sulfate formation across the domain (Fig. 1). The highest $f_{\text{S(IV)}+\text{O}_3}$ occurs in the Western States, due to the high O_3 concentration and high cloud pH (Fig. S1), which facilitate the aqueous oxidation of S(IV) by O_3 . With a higher $\Delta^{17}\text{O}(\text{ASO}_4)$ value resulting from the S(IV) + O_3 pathway of 6.5‰, the higher $f_{\text{S(IV)}+\text{O}_3}$ in these regions results in elevated $\Delta^{17}\text{O}(\text{ASO}_4)$ values, typically above 3‰. Minor pathways, such as those involving TMI, MHP, and PAA, contribute 3.4%, 0.37%, and 0.26%, respectively (Fig. 1), to sulfate formation across the
200 US continuous domain. Similarly, gas-phase oxidation of SO_2 by OH is negligible, accounting for only 0.2% of the total sulfate production (Fig. 1). Primary sulfate emissions account for 20.9% of total sulfate production (Fig. 1), with substantial contributions originating from urban and industrial regions. While high SO_2 emissions from anthropogenic activities in these areas elevate the role of primary sulfate, their impact on $\Delta^{17}\text{O}(\text{ASO}_4)$ values remains spatially limited.

205 Cloud pH is a critical determinant of ASO_4 formation pathways and $\Delta^{17}\text{O}(\text{ASO}_4)$ values, with lower cloud pH favoring the H_2O_2 pathway and higher cloud pH supporting the O_3 pathway. The concentration of ASO_4 plays a dominant role in lowering cloud pH, primarily due to its origin from sulfuric acid (H_2SO_4). As a strong acid, H_2SO_4 dissociates completely, releasing significant amounts of hydrogen ions (H^+) and causing substantial acidification of cloud water. In regions such as the Northeast, Southeast, and Midwest, relatively high SO_2 emissions lead to elevated ASO_4 concentrations (Fig. S1). This is
210 due to the efficient conversion of SO_2 to ASO_4 . These high ASO_4 levels contribute significantly to lowering cloud pH in these areas, creating an acidic environment (Fig. S1). In contrast, in the Western States, SO_2 emissions and ASO_4 concentrations are comparatively lower (Fig. S1). This results in reduced acidification and a higher cloud pH, as the influence of sulfate on the acidity of cloud water is diminished. Ammonium in cloud water (ANH_4), on the other hand, primarily acts as a buffering agent, mitigating the acidity caused by sulfate (Fig. S1). NH_3 reacts with H_2SO_4 to form
215 $(\text{NH}_4)_2\text{SO}_4$ (ammonium sulfate), which reduces the availability of free H^+ and partially neutralizes the acidification caused by ASO_4 . However, the neutralizing capacity of ANH_4 is limited. In regions with high ASO_4 concentrations, such as the Northeast and Southeast, the buffering effect of ANH_4 is insufficient to fully counteract the strong acidity introduced by



ASO₄. In the Midwest, where NH₃ emissions from agricultural activities, particularly fertilization, are significant, the resulting high concentrations of ANH₄ partially neutralize the acidity from ASO₄ (Fig. S1). This interaction raises cloud pH slightly, preventing extreme acidification (Fig. S1). Nevertheless, even in regions with abundant NH₃ emissions, cloud water pH typically remains acidic because of the dominant influence of ASO₄. The strong acidity introduced by ASO₄ sets a baseline pH, limiting the extent to which ammonium can mitigate acidification. Therefore, ASO₄ plays a primary role in determining cloud water pH through its strong acidifying effect, particularly in regions with high SO₂ emissions. While ANH₄ can buffer acidity and raise pH to some extent, its influence is secondary to that of ASO₄. The interplay between these species shapes the chemical environment of cloud water and determines the pathways for ASO₄ formation.

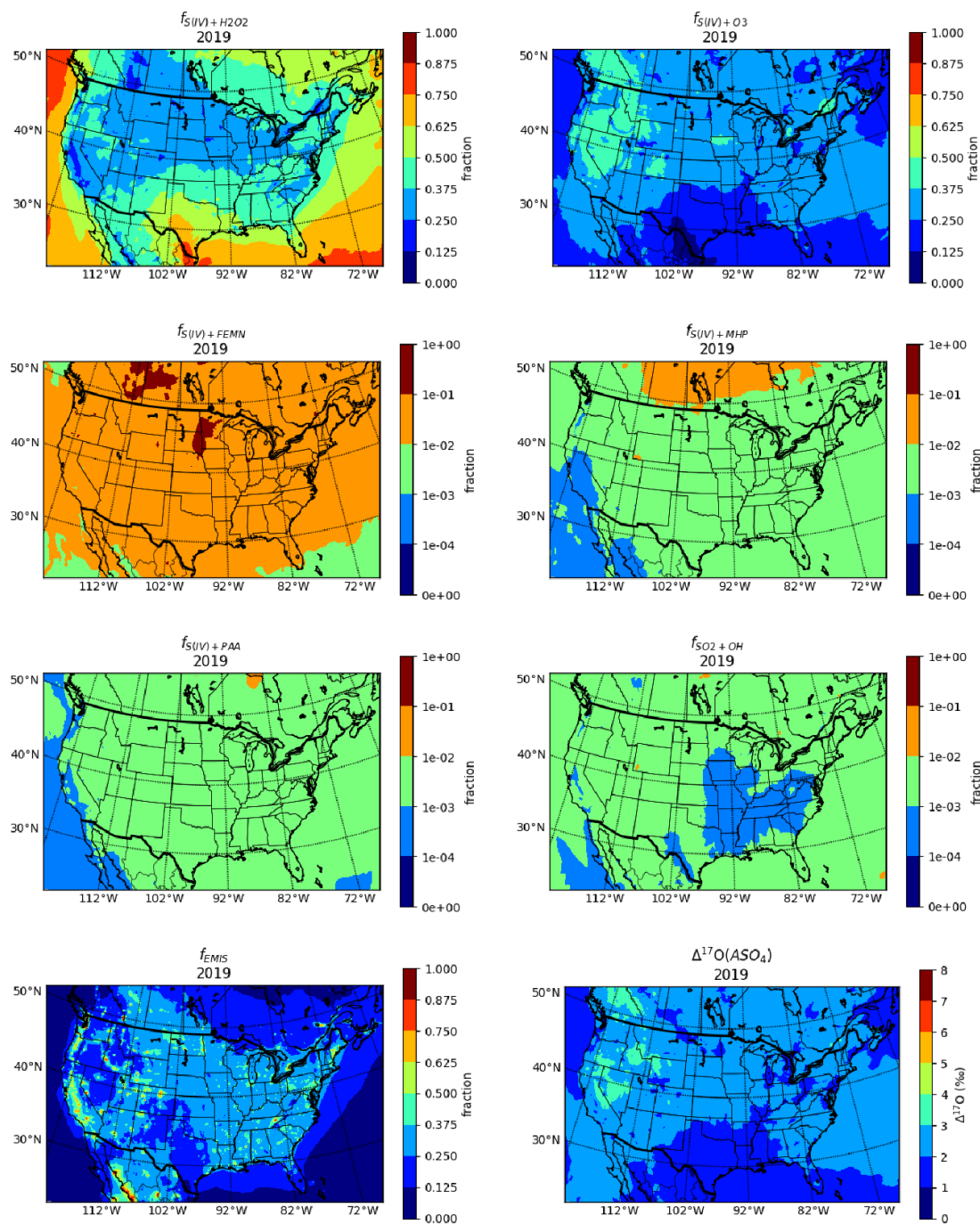


Fig. 1: The geographical distribution of the fraction from each SO_4^{2-} formation pathway, along with $\Delta^{17}\text{O}$ values across the continental US in the year 2019, based on CMAQ simulation.



3.2 Seasonal Variation in Fractional ASO₄ Formation and $\Delta^{17}\text{O}(\text{ASO}_4)$ in the Contiguous US in 2019

Sulfate formation across the contiguous United States exhibits distinct seasonal patterns, shaped by varying contributions from the H₂O₂ and O₃ pathways, as well as shifts in cloud pH and precursor concentrations (Fig. S1). The isotopic composition of ASO₄, represented by $\Delta^{17}\text{O}(\text{ASO}_4)$, reflects the dominance of specific pathways under different meteorological and chemical conditions. In regions with low cloud pH, the H₂O₂ pathway dominates, resulting in low $\Delta^{17}\text{O}$ values (Fig. S1, Fig. 2). Conversely, areas with high cloud pH favor the O₃ pathway, resulting in high $\Delta^{17}\text{O}$ values (Fig. S1, Fig. 2). Seasonal changes in cloud pH, ASO₄, and ANH₄ (Fig. S3, Fig. S4, Fig. S6) further influence these trends, highlighting the complex interplay of emissions, atmospheric chemistry, and meteorology.

In January, the Western States exhibit the highest $\Delta^{17}\text{O}(\text{ASO}_4)$ values, exceeding 2‰ (Fig. 2). This is driven by the dominance of the O₃ pathway (Fig. 3), supported by elevated cloud pH levels resulting from low ASO₄ concentrations (Fig. S3, Fig. S4). Conversely, the Gulf Coast States show the lowest $\Delta^{17}\text{O}(\text{ASO}_4)$ values, typically below 1‰ (Fig. S1), primarily due to the prevalence of the H₂O₂ pathway (Fig. 4). This pathway dominates under low cloud pH conditions caused by high ASO₄ concentrations and limited ANH₄ levels (Fig. S3, Fig. S4, Fig. S6). In the Midwest, moderate $\Delta^{17}\text{O}(\text{ASO}_4)$ values are shown, reflecting a balance between pathways. Elevated ANH₄ levels partially neutralize the acidity from high ASO₄ concentrations (Fig. S4, Fig. S6). This neutralization raises cloud pH (Fig. S3), diminishing the dominance of the H₂O₂ pathway (Fig. 4) and contributing to the intermediate $\Delta^{17}\text{O}(\text{ASO}_4)$ values.

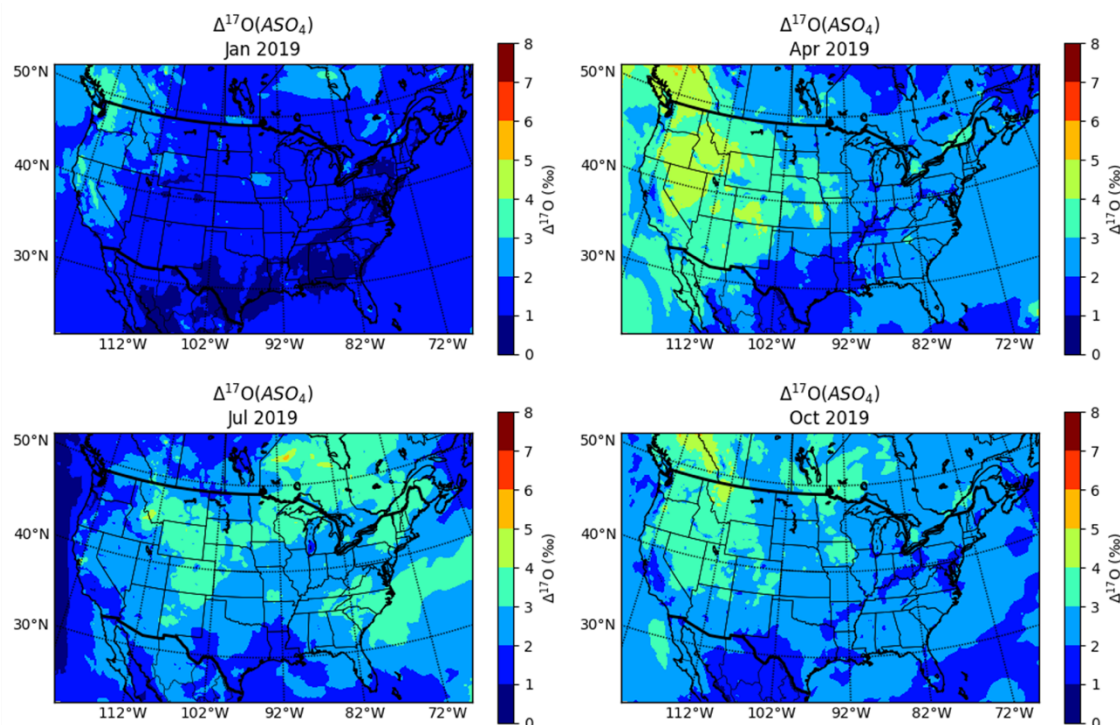
In April, $\Delta^{17}\text{O}$ values increase significantly, particularly in the Western States, rising above 3‰ (Fig. 2). This trend indicates an enhanced influence of the O₃ pathway, supported by elevated cloud pH and increased O₃ levels (Fig. 3, Fig. S3, Fig. S8). In contrast, the Gulf Coast States continue to exhibit low $\Delta^{17}\text{O}$ values (< 2‰) (Fig. 2), as the H₂O₂ pathway remains dominant due to persistently low cloud pH (Fig. 4, Fig. S3). This acidity is driven by high ASO₄ concentrations and low ANH₄ concentrations (Fig. S4, Fig. S6). Meanwhile, in the Midwest, cloud pH begins to rise as increased NH₃ levels, partially neutralizing the acidity from ASO₄ and shifting the balance of sulfate formation pathways (Fig. S3, Fig. S4, Fig. S7).

In July, $\Delta^{17}\text{O}$ values decrease in the Western States as the $f_{S(\text{IV})+\text{H}_2\text{O}_2}$ increases compared to April (Fig. 2). This shift is driven by higher water vapor levels and increased cloud cover (Fig. S10), despite the region's consistently high cloud pH (Fig. S3). In the Gulf Coast States, $\Delta^{17}\text{O}$ values remain low, below 2‰ (Fig. S1), highlighting the continued dominance of the H₂O₂ pathway (Fig. 4) under conditions of abundant water vapor (Fig. S10), frequent cloud cover (Fig. S11), and persistently low cloud pH (Fig. S3). In the Midwest, cloud pH continues to rise from April (Fig. S3), driven by increasing NH₃ concentrations (Fig. S7), which partially neutralize the acidity caused by ASO₄ (Fig. S4). This elevation in cloud pH enhances the activity of the O₃ pathway (Fig. S2), leading to an increase in $\Delta^{17}\text{O}$ values compared to April.



In October, $\Delta^{17}\text{O}$ values in the Western States increase compared to July but remain slightly lower than in April (Fig. 2).
 265 This change is attributed to the enhanced $f_{S(IV)+O_3}$ (Fig. S2), supported by high cloud pH and low ASO_4 concentrations (Fig. S3, Fig. S4). In the Gulf Coast States, $\Delta^{17}\text{O}$ values remain low (Fig. 2), reflecting the continued dominance of the H_2O_2 pathway under acidic conditions sustained by high ASO_4 levels and low NH_3 concentrations (Fig. S3, Fig. S4, Fig. S6). In the Midwest, decreasing NH_3 levels from July reduce the neutralization of acidity (Fig. S3, Fig. S7), making conditions less favorable for ozone-driven sulfate formation (Fig. 3). This results in lower cloud pH (Fig. S3) and diminished $\Delta^{17}\text{O}$ values
 270 compared to earlier months.

Seasonal variations in sulfate formation and $\Delta^{17}\text{O}(\text{ASO}_4)$ highlight the interplay of chemical drivers and meteorological conditions. The dominance of the H_2O_2 pathway in acidic, ASO_4 -rich regions like the Gulf Coast States leads to low $\Delta^{17}\text{O}$ values year-round. In contrast, the O_3 pathway prevails in higher pH regions such as the Western States, driving elevated
 275 $\Delta^{17}\text{O}$ values, particularly in April. The Midwest experience transitional conditions, where cloud pH and NH_3 concentrations modulate the relative contributions of ASO_4 formation pathways. These findings underscore the dynamic nature of sulfate chemistry across seasons, emphasizing the importance of emissions, atmospheric composition, and cloud chemistry in shaping regional and seasonal patterns of sulfate formation.



280



Fig. 2: The geographical distribution of $\Delta^{17}\text{O}$ values across the continental US for the year 2019 in each season (winter: Jan, spring: Apr, summer: July, fall: Oct), based on CMAQ simulation.

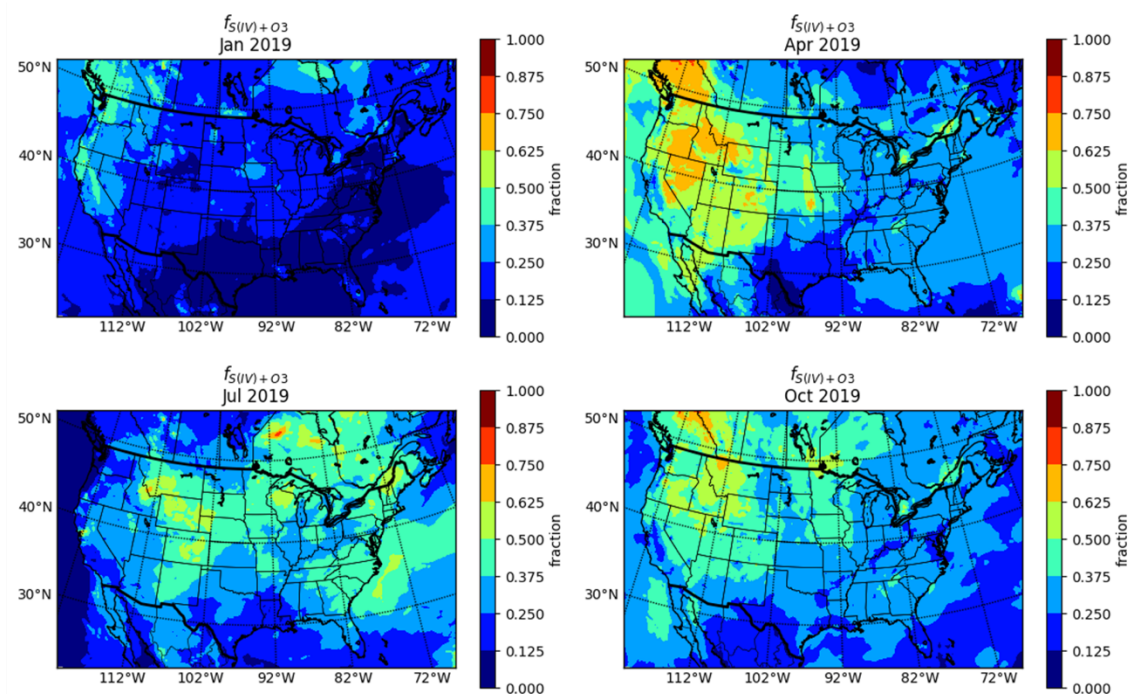
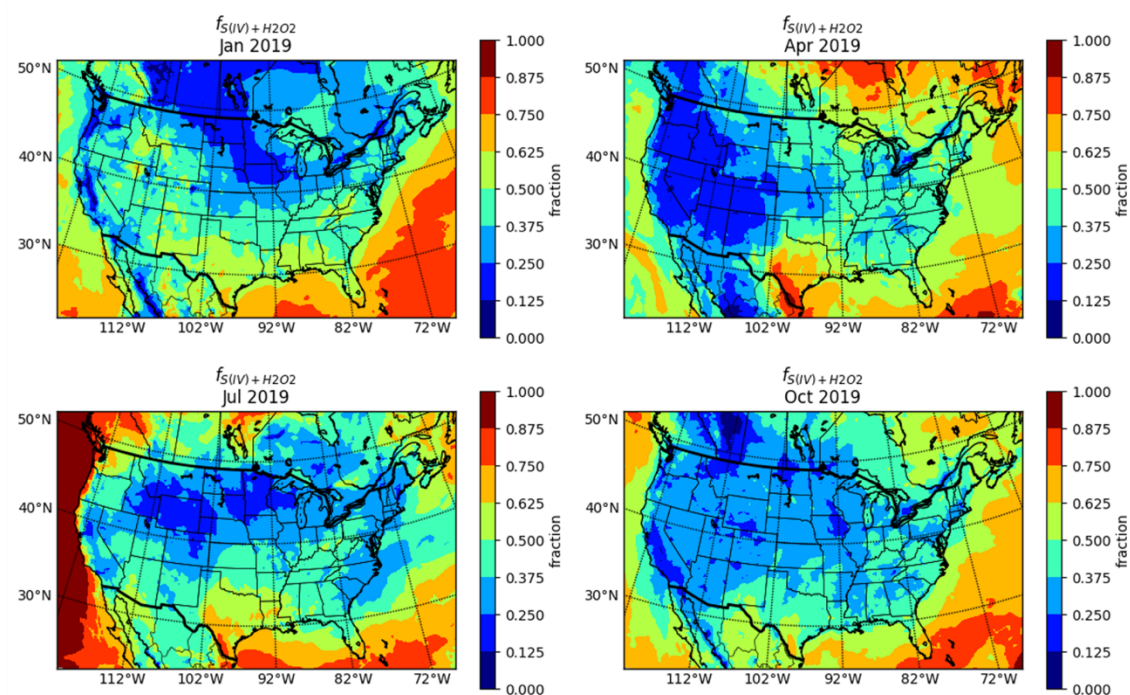


Fig. 3: The geographical distribution of the fraction of SO_4^{2-} formation from $\text{S(IV)} + \text{O}_3$ pathway across the continental US for the year 2019 in each season (winter: Jan, spring: Apr, summer: July, fall: Oct), based on CMAQ simulation.



290 **Fig. 4: The geographical distribution of the fraction of SO_4^{2-} formation from $\text{S(IV)} + \text{H}_2\text{O}_2$ pathway across the continental US for the year 2019 in each season (winter: Jan, spring: Apr, summer: July, fall: Oct), based on CMAQ simulation.**

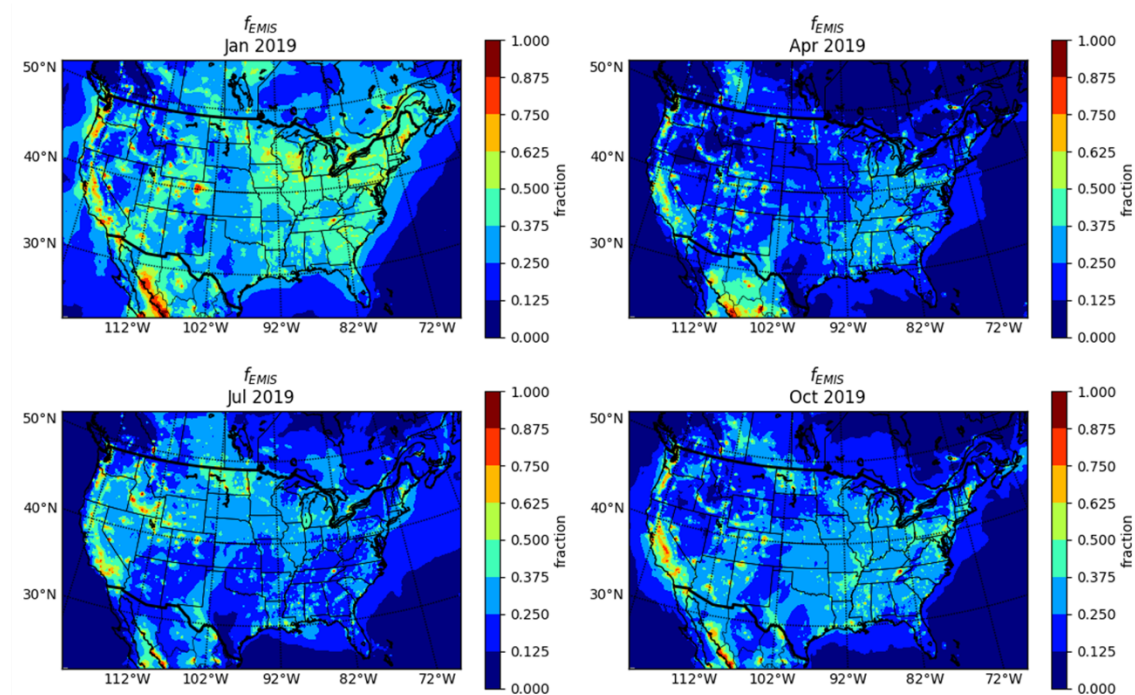


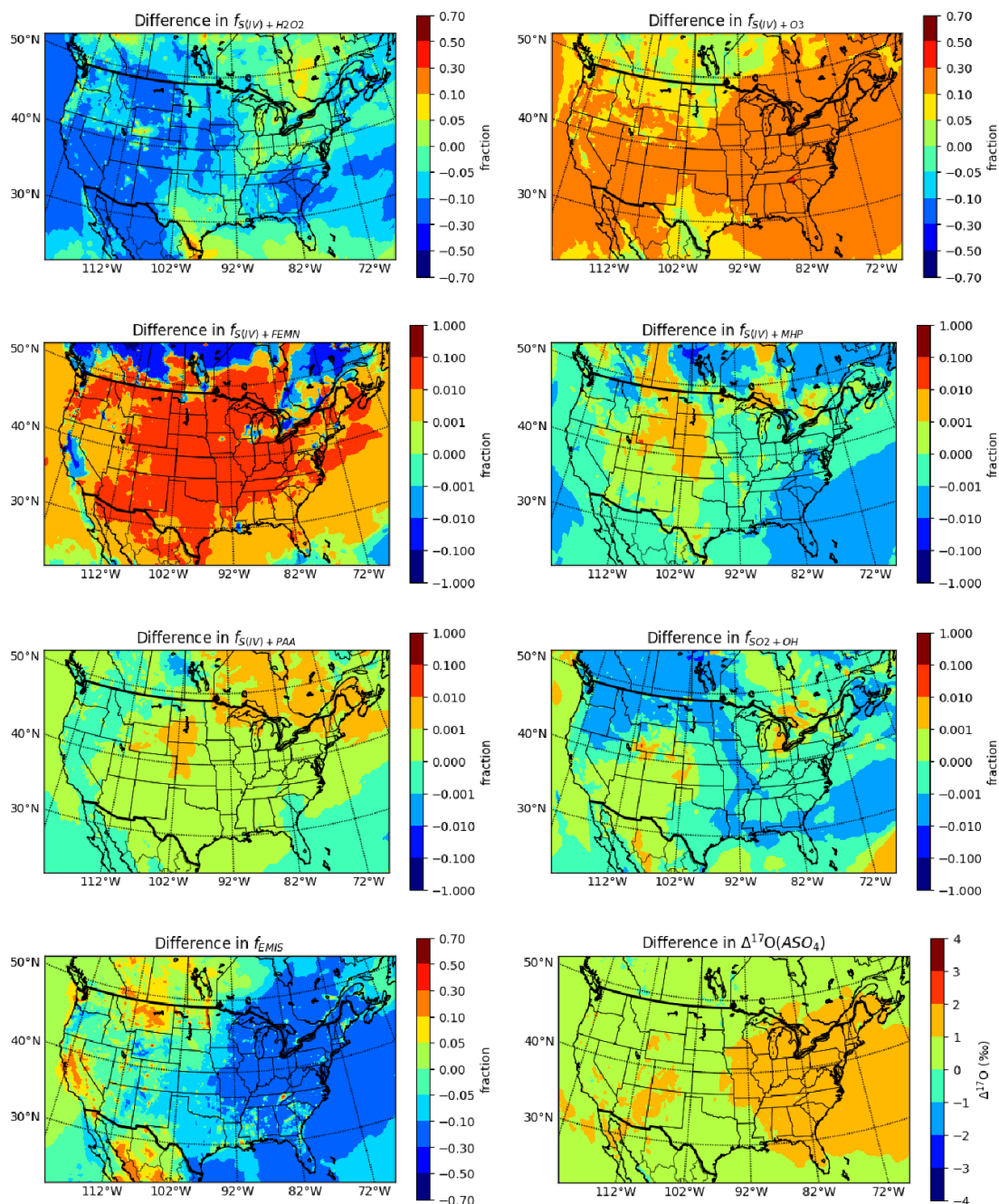
Fig. 5: The geographical distribution of the fraction of SO_4^{2-} formation from primary emission across the continental US for the year 2019 in each season (winter: Jan, spring: Apr, summer: July, fall: Oct), based on CMAQ simulation.

3.3 Change in Fractional Annual ASO_4 Formation and $\Delta^{17}\text{O}(\text{ASO}_4)$ from 2006 to 2019

From 2006 to 2019, the annual $\Delta^{17}\text{O}(\text{ASO}_4)$ values across the contiguous US showed a consistent increase, highlighting the growing dominance of the O_3 pathway in ASO_4 formation (Fig. 6). In the central and eastern US, $\Delta^{17}\text{O}(\text{ASO}_4)$ values increased by up to 2‰ (Fig. 6), primarily driven by significant reductions in SO_2 emissions, largely attributable to regulatory measures such as the Clean Air Act. These reductions led to lower ASO_4 concentrations, which elevated cloud pH and shifted the sulfate formation process toward the O_3 pathway (Fig. S12), producing ASO_4 with a higher $\Delta^{17}\text{O}$ values. Conversely, the western US exhibited only modest increases in $\Delta^{17}\text{O}(\text{ASO}_4)$, typically less than 1‰ (Fig. 6). This is because the region historically favored O_3 -dominated ASO_4 formation due to consistently high O_3 and cloud pH levels (Fig. S13), making the impacts of rising cloud pH and reduced SO_2 emissions less pronounced. Changes in H_2O_2 concentrations played a significant role in shaping these trends. In the central and eastern US, slight increases in H_2O_2 concentrations continued to support the H_2O_2 pathway, to a limited extent, even as the O_3 pathway became more dominant (Fig. 6, Fig. S12). In contrast, in the western US, H_2O_2 concentrations decreased slightly, resulting in a more pronounced reduction in $f_{S(\text{IV})+\text{H}_2\text{O}_2}$ (Fig. 6). Given the negligible contributions from other pathways, this shift caused a relative increase in f_{EMIS} in these regions (Fig. 6). Primary sulfate emissions, which are not subject to isotopic fractionation, directly added to sulfate levels and tempered



changes in $\Delta^{17}\text{O}(\text{ASO}_4)$ values (Fig. 6). This dynamic explains why the increases in $\Delta^{17}\text{O}(\text{ASO}_4)$ values from 2006 to 2019 were smaller in the western US compared to the central and eastern regions.



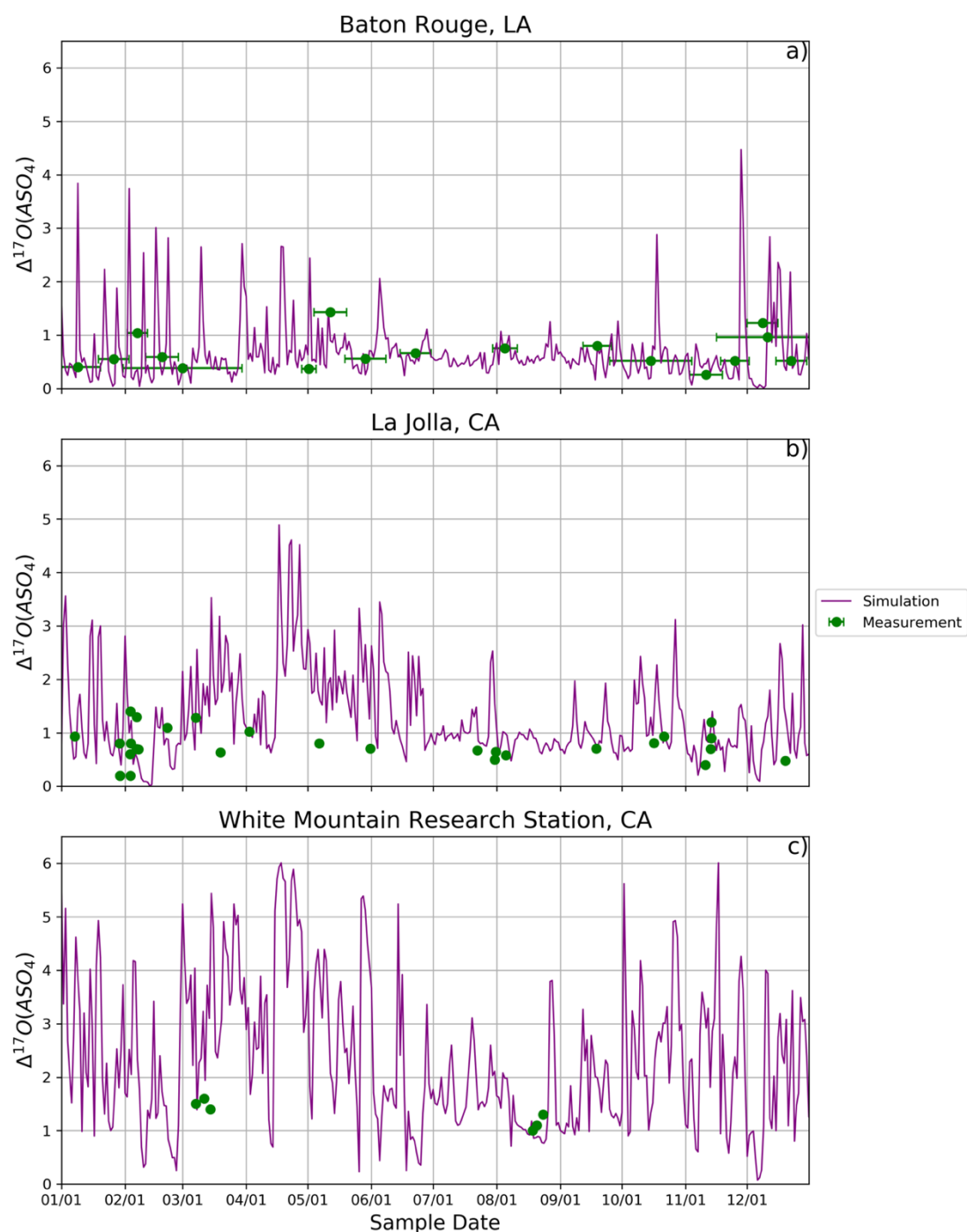


315 **Fig. 6: The geographical distribution of the change in the fraction from each SO_4^{2-} formation pathway and $\Delta^{17}\text{O}$ values across the continental US, from 2006 to 2019, based on CMAQ simulation.**

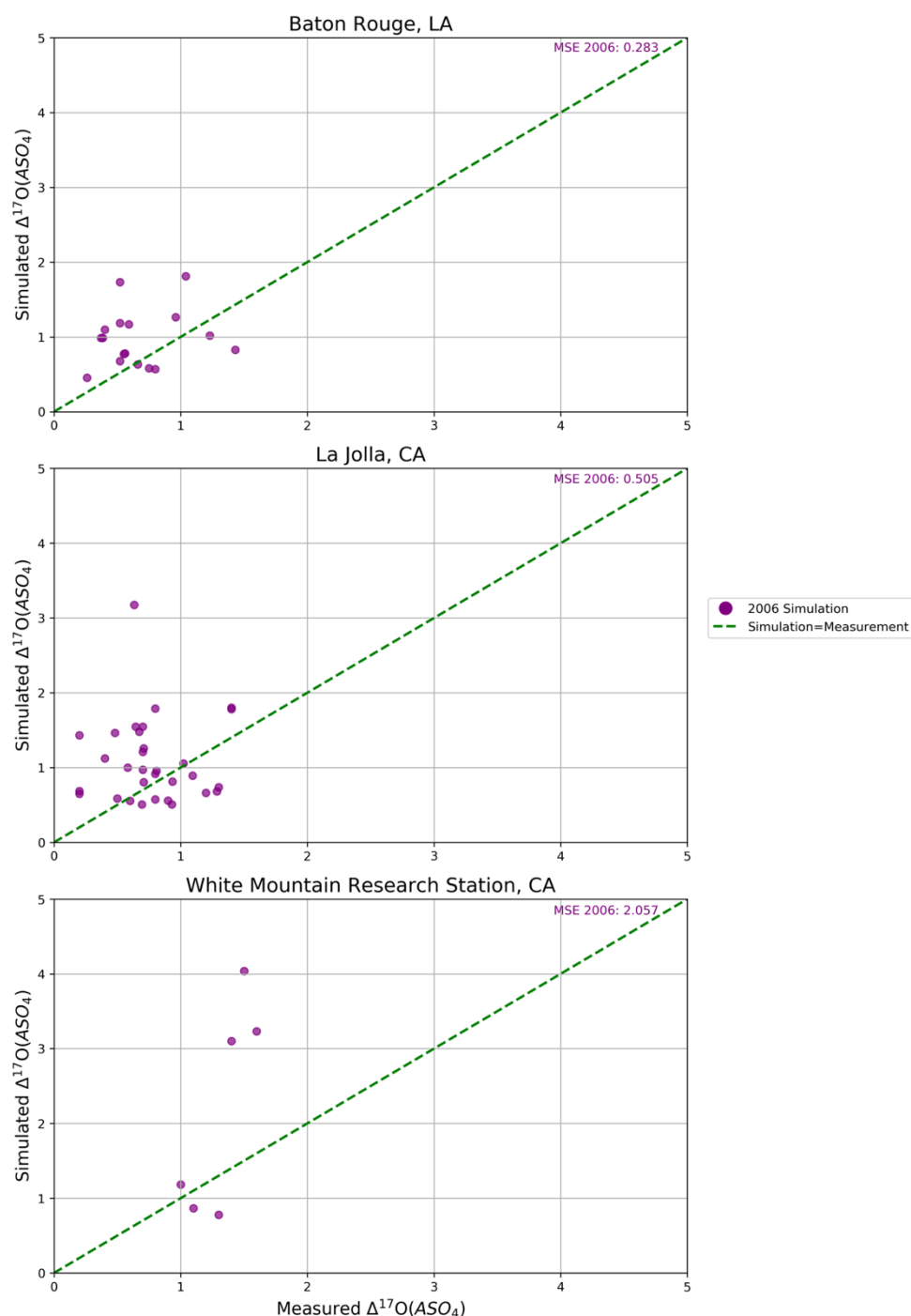
3.4 Comparison of Model $\Delta^{17}\text{O}(\text{ASO}_4)$ with Observations

320 The CMAQ simulations of $\Delta^{17}\text{O}(\text{ASO}_4)$ across the contiguous United States reveals significant insights into atmospheric sulfate formation over recent decades. However, observations of $\Delta^{17}\text{O}$ in the contiguous US are very limited, with data primarily collected in the late 1990s at La Jolla, CA, and White Mountain Research Station, CA (Lee & Thiemens, 2001), and in the early 2000s at Baton Rouge, LA (Jenkins & Bao, 2006). These historical $\Delta^{17}\text{O}$ data exhibit a range from 0.2‰ to 1.6‰ (Table S1). Due to the predicted change in ASO_4 chemistry from 2006 to 2019, the 2006 model simulation was chosen for evaluation against these observations (Fig. 7, 8).

325 Generally, the CMAQ model reasonably reproduced $\Delta^{17}\text{O}(\text{ASO}_4)$ at the Baton Rouge, LA site, with a Root Mean Square Error (RMSE) of 0.283‰ ($n=17$). This region is characterized by low predicted $\Delta^{17}\text{O}(\text{ASO}_4)$ values due to high regional SO_2 emissions and low cloud water pH, which favor ASO_4 formation via aqueous $\text{S(IV)} + \text{H}_2\text{O}_2$ reactions. In contrast, the CMAQ-simulated $\Delta^{17}\text{O}(\text{ASO}_4)$ values tended to be overestimated at the California sites, suggesting inaccuracies in
330 representing additional sulfate production pathways in this region. The La Jolla, CA site had an RMSE of 0.505‰ ($n=31$), while the White Mountain, CA site had a notably higher RMSE of 2.1‰ ($n=6$). Despite the limited number of $\Delta^{17}\text{O}(\text{ASO}_4)$ observations, a temporal analysis of model simulations versus observations indicates a persistent overprediction during the spring (Fig. 8). This period coincides with elevated NH_3 emissions from fertilization (Fig. S26), which can increase cloud pH and shift aqueous-phase S(IV) oxidation toward the O_3 pathway under high-pH conditions, leading to higher $\Delta^{17}\text{O}(\text{ASO}_4)$
335 values. These findings suggest that the CMAQ model may misrepresent NH_3 emissions or their impact on cloud pH, which has a significant influence on sulfate chemistry. Additionally, certain sulfate formation pathways, such as marine boundary layer chemistry involving S(IV) oxidation by HOX, may not be fully captured, particularly at coastal sites like La Jolla, CA. Overall, the model-observation comparison of $\Delta^{17}\text{O}(\text{ASO}_4)$ suggests that CMAQ performs well in more acidic environments but struggles to accurately simulate sulfate formation under less acidic conditions. However, the limited availability of
340 $\Delta^{17}\text{O}(\text{ASO}_4)$ observations constrains a more comprehensive evaluation of regional and temporal sulfate chemistry variations. This highlights the critical need for expanded observational datasets and model refinements to better represent the complex atmospheric sulfate dynamics.



345 **Fig. 7: Temporal variations in $\Delta^{17}\text{O}(\text{ASO}_4)$ measurements and model simulations at a). Baton Rouge, LA (top); b) La Jolla, CA (middle); and c) White Mountain Research Station, CA (bottom). The x-axis error bars correspond to collection times.**



350 **Fig. 8: Comparison of $\Delta^{17}\text{O}(\text{ASO}_4)$ measurements and model simulations at La Jolla, CA, White Mountain Research Station, CA, and Baton Rouge, LA from 1996 to 2005.**



4 Conclusions

This study modeled ASO_4 formation pathways and the $\Delta^{17}\text{O}(\text{ASO}_4)$ for the contiguous United States using the CMAQ model for 2006 and 2019. The results reveal distinct seasonal and regional patterns in sulfate chemistry, strongly influenced by photochemical conditions, emissions of SO_2 and NH_3 , and variations in cloud pH. From 2006 to 2019, significant changes in sulfate formation dynamics were observed, driven primarily by regulatory-driven reductions in SO_2 emissions. These shifts highlight the evolving balance between aqueous-phase oxidation pathways, particularly those driven by H_2O_2 and O_3 .

The reductions in SO_2 emissions due to the Clean Air Act resulted in lower cloud water ASO_4 , which subsequently increased cloud pH. This change shifted sulfate production toward the O_3 pathway, particularly in the eastern US, where the O_3 pathway was once limited by lower pH levels in 2006. By 2019, sulfate formation via O_3 oxidation had increased significantly, indicating a more efficient production mechanism under elevated pH conditions. The sub-linear response of ASO_4 concentrations to SO_2 emission reductions underscores the complexity of sulfate formation chemistry and the role of co-emitted species like NH_3 in modifying pH levels and pathway dominance.

The isotopic signature $\Delta^{17}\text{O}(\text{ASO}_4)$ serves as a powerful tracer for tracking shifts in sulfate formation pathways. In regions with limited photochemical activity, such as during winter or in areas with high primary sulfate emissions, lower $\Delta^{17}\text{O}$ values were associated with greater contributions from primary ASO_4 emissions. Conversely, higher $\Delta^{17}\text{O}$ values reflected an increased role of the O_3 pathway, particularly in regions with elevated cloud pH, reduced SO_2 emissions, and higher ozone concentrations.

This work demonstrates a significant and predictable shift in sulfate chemistry over the study period. The introduction of $\Delta^{17}\text{O}(\text{ASO}_4)$ as a diagnostic tool for probing ASO_4 formation mechanisms provides a novel approach for investigating these changes. Expanding the measurement of $\Delta^{17}\text{O}(\text{ASO}_4)$ across diverse regions and time periods will be critical for validating and extending these findings. Future studies should prioritize exploring how changes in atmospheric composition and regulatory measures continue to influence ASO_4 chemistry, with a particular focus on understanding the increasing prominence of O_3 -driven chemistry. This effort will be essential for improving atmospheric models and addressing the implications of sulfate chemistry on air quality, human health, and climate.

Code and Data Availability: The source code for CMAQ version 5.4 is available at <https://github.com/USEPA/CMAQ/tree/5.4> (last access: 1 March 2025). The input datasets for CMAQ simulation are available at https://cmas-equates.s3.amazonaws.com/index.html#CMAQ_12US1/INPUT/ (last access: 1 March 2025). The



in-detail simulation results for $\Delta^{17}\text{O}(\text{ASO}_4)$ are achieved on Zenodo.org (<https://doi.org/10.5281/zenodo.14954960>, Fang,
385 2025).

Author contributions: HF and WWW designed the study. HF conducted the model simulations and analysis with input from WWW. HF wrote the manuscript with input from all authors. WWW secured funding.

390 **Competing Interests:** The contact author has declared that none of the authors have competing interests.

Acknowledgements: We thank Kristen Foley for providing the base model input files. We thank Myk Milligan and Nathan Elger and the staff of the Hyperion cluster for helping to install CMAQ, transferring data, and maintenance of the computing cluster

395

Financial Support: This research has been supported by NSF AGS (2414561), NSF EPSCOR RII Track-4 (2410015), and USC start-up funds.



400 References

- Alexander, B., Park, R. J., Jacob, D. J., & Gong, S.: Transition metal-catalyzed oxidation of atmospheric sulfur: Global implications for the sulfur budget. *Journal of Geophysical Research: Atmospheres*, 114(D2), doi:10.1029/2008JD010486, 2009.
- Alexander, B., Park, R. J., Jacob, D. J., Li, Q. B., Yantosca, R. M., Savarino, J., Lee, C. C. W., & Thiemens, M. H.: Sulfate
405 formation in sea-salt aerosols: Constraints from oxygen isotopes. *Journal of Geophysical Research*, 110, D10307, doi:10.1029/2004JD005659, 2005.
- Alexander, B., Savarino, J., Kreutz, K. J., & Thiemens, M. H.: Impact of preindustrial biomass-burning emissions on the oxidation pathways of tropospheric sulfur and nitrogen. *Journal of Geophysical Research*, 109, D08303, doi:10.1029/2003JD004218, 2004.
- 410 Appel, K. W., Bash, J. O., Fahey, K. M., Foley, K. M., Gilliam, R. C., Hogrefe, C., ... & Wong, D. C.: The Community Multiscale Air Quality (CMAQ) model versions 5.3 and 5.3. 1: system updates and evaluation. *Geoscientific Model Development*, 14(5), 2867-2897, doi:10.5194/gmd-14-2867-2021, 2021.
- Arimoto, R., Nottingham, A. S., Webb, J., Schloesslin, C. A., & Davis, D. D.: Non-sea salt sulfate and other aerosol constituents at the South Pole during ISCAT. *Geophysical Research Letters*, 28(19), 36453648, doi:10.1029/2000GL012714,
415 2001.
- Barkan, E., & Luz, B.: High-precision measurements of $^{17}\text{O}/^{16}\text{O}$ and $^{18}\text{O}/^{16}\text{O}$ of O_2 and O_2/Ar ratio in air. *Rapid Communications in Mass Spectrometry*, 17(24), 28092814, doi:10.1002/rcm.1267, 2003.
- Benish, S. E., Bash, J. O., Foley, K. M., Appel, K. W., Hogrefe, C., Gilliam, R., & Pouliot, G.: Long-term regional trends of nitrogen and sulfur deposition in the United States from 2002 to 2017. *Atmospheric Chemistry and Physics*, 22(19), 12749-
420 12767, doi:10.5194/acp-22-12749-2022, 2022.
- Bhattacharya, S. K., Pandey, A., & Savarino, J.: Determination of intramolecular isotope distribution of ozone by oxidation reaction with silver metal. *Journal of Geophysical Research: Atmospheres*, 113(D3), doi:10.1029/2006JD008309, 2008.
- Bianchi, F., Kurtén, T., Riva, M., Mohr, C., Rissanen, M. P., Roldin, P., ... & Ehn, M.: Highly oxygenated organic molecules (HOM) from gas-phase autoxidation involving peroxy radicals: A key contributor to atmospheric aerosol. *Chemical reviews*,
425 119(6), 3472-3509, doi:10.1021/acs.chemrev.8b00395, 2019.
- Calvo, A. I., Alves, C., Castro, A., Pont, V., Vicente, A. M., & Fraile, R.: Research on aerosol sources and chemical composition: Past, current and emerging issues. *Atmospheric Research*, 120, 1-28, doi:10.1016/j.atmosres.2012.09.021, 2013.
- Chen, Q., Geng, L., Schmidt, J. A., Xie, Z., Kang, H., Dachs, J., ... & Alexander, B.: Isotopic constraints on the role of hypohalous acids in sulfate aerosol formation in the remote marine boundary layer. *Atmospheric Chemistry and Physics*,
430 16(17), 11433-11450, doi:10.5194/acp-16-11433-2016, 2016.



- Dominguez, G., Jackson, T., Brothers, L., Barnett, B., Nguyen, B., & Thiemens, M. H.: Discovery and measurement of an isotopically distinct source of sulfate in Earth's atmosphere. *Proceedings of the National Academy of Sciences*, 105(35), 12,769-12,773, doi:10.1073/pnas.0805255105, 2008.
- Fang, H.: Simulating $\Delta^{17}\text{O}$ of sulfate aerosol within the contiguous United States to trace the formation processes, Zenodo [data set], doi:10.5281/zenodo.14954960, 2025.
- Foley, K. M., Pouliot, G. A., Eyth, A., Aldridge, M. F., Allen, C., Appel, K. W., ... & Adams, E.: 2002-2017 anthropogenic emissions data for air quality modeling over the United States. *Data in Brief*, 47, 109022, doi:10.1016/j.dib.2023.109022, 2023
- Hallquist, M., Wenger, J. C., Baltensperger, U., Rudich, Y., Simpson, D., Claeys, M., ... & Wildt, J.: The formation, properties and impact of secondary organic aerosol: current and emerging issues. *Atmospheric chemistry and physics*, 9(14), 5155-5236, doi:10.5194/acp-9-5155-2009, 2009.
- Harris, E., Sinha, B., Van Pinxteren, D., Tilgner, A., Fomba, K. W., Schneider, J., ... & Herrmann, H.: Enhanced role of transition metal ion catalysis during in-cloud oxidation of SO_2 . *science*, 340(6133), 727-730, doi:10.1126/science.1230911, 2013
- Haywood, J., & Boucher, O. (2000). Estimates of the direct and indirect radiative forcing due to tropospheric aerosols: A review of Geophysics, 38(4), 513-543, doi:10.1029/1999RG000078, 2000.
- Ishino, S., Hattori, S., Savarino, J., Jourdain, B., Preunkert, S., Legrand, M., et al.: Seasonal variations of triple oxygen isotopic compositions of atmospheric sulfate, nitrate, and ozone at Dumont d'Urville, coastal Antarctica. *Atmospheric Chemistry and Physics*, 17(5), 3713-3727, doi:10.5194/acp-17-3713-2017, 2017.
- Jenkins, K. A., & Bao, H.: Multiple oxygen and sulfur isotope compositions of atmospheric sulfate in Baton Rouge, LA, USA. *Atmospheric Environment*, 40(24), 4528-4537, doi:10.1016/j.atmosenv.2006.04.010, 2006.
- Jones, A. D. L. A., Roberts, D. L., & Slingo, A.: A climate model study of indirect radiative forcing by anthropogenic sulphate aerosols. *Nature*, 370(6489), 450-453, doi:10.1038/370450a0, 1994.
- Kaiser, J., Röckmann, T., & Brenninkmeijer, C. A.: Contribution of mass-dependent fractionation to the oxygen isotope anomaly of atmospheric nitrous oxide. *Journal of Geophysical Research*, 109, D033055, doi:10.1029/2003JD004088, 2004.
- Kaufman, Y. J., & Tanré, D.: Effect of variations in super-saturation on the formation of cloud condensation nuclei. *Nature*, 369(6475), 45-48, doi:10.1038/369045a0, 1994.
- Langner, J., Rodhe, H., Crutzen, P. J., & Zimmermann, P.: Anthropogenic influence on the distribution of tropospheric sulphate aerosol. *Nature*, 359(6397), 712-716, doi:10.1038/359712a0, 1992.
- Lee, C. C. W., & Thiemens, M. H.: The $\delta^{17}\text{O}$ and $\delta^{18}\text{O}$ measurements of atmospheric sulfate from a coastal and high alpine region: A mass independent isotopic anomaly. *Journal of Geophysical Research: Atmospheres*, 106(D15), 17359-17373, doi:10.1029/2000JD900805, 2001.



- Li, J., Zhang, Y. L., Cao, F., Zhang, W., Fan, M., Lee, X., & Michalski, G.: Stable sulfur isotopes revealed a major role of transition-metal ion-catalyzed SO₂ oxidation in haze episodes. *Environmental Science & Technology*, 54(5), 2626-2634, doi:10.1021/acs.est.9b07150, 2020.
- Liang, J., & Jacobson, M. Z.: A study of sulfur dioxide oxidation pathways over a range of liquid water contents, pH values, and temperatures. *Journal of Geophysical Research*, 104(D11), 13,749-13,769, doi:10.1029/1999JD900097, 1999.
- Liu, L., Bei, N., Wu, J., Liu, S., Zhou, J., Li, X., ... & Li, G.: Effects of stabilized Criegee intermediates (sCIs) on sulfate formation: a sensitivity analysis during summertime in Beijing–Tianjin–Hebei (BTH), China. *Atmospheric Chemistry and Physics*, 19(21), 13341-13354, doi:10.5194/acp-19-13341-2019, 2019.
- Lohmann, U., & Feichter, J.: Impact of sulfate aerosols on albedo and lifetime of clouds: A sensitivity study with the ECHAM4 GCM. *Journal of Geophysical Research: Atmospheres*, 102(D12), 13685-13700, doi:10.1029/97JD00631, 1997.
- Meidan, D., Holloway, J. S., Edwards, P. M., Dube, W. P., Middlebrook, A. M., Liao, J., ... & Rudich, Y.: Role of Criegee intermediates in secondary sulfate aerosol formation in nocturnal power plant plumes in the Southeast US. *ACS Earth and Space Chemistry*, 3(5), 748-759, doi:10.1021/acsearthspacechem.8b00215, 2019.
- Michalski, G. M., Scott, Z., Kabling, M., and Thiemens, M. H.: First measurements and modeling of ¹⁷O in atmospheric nitrate, *Geophys. Res. Lett.*, 30, 1870, doi:10.1029/2003GL017015, 2003.
- Morin, S., Savarino, J., Bekki, S., Gong, S., & Bottenheim, J. W.: Signature of Arctic surface ozone depletion events in the isotope anomaly (¹⁷O) of atmospheric nitrate. *Atmospheric Chemistry and Physics*, 7(5), 1451-1469, doi:10.5194/acp-7-1451-2007, 2007.
- Pandis, S. N., & Seinfeld, J. H.: Sensitivity analysis of a chemical mechanism for aqueous-phase atmospheric chemistry. *Journal of Geophysical Research*, 94(D1), 11051-1126, doi:10.1029/JD094iD01p01105, 1989.
- Reiss, R., Anderson, E. L., Cross, C. E., Hidy, G., Hoel, D., McClellan, R., & Moolgavkar, S.: Evidence of health impacts of sulfate-and nitrate-containing particles in ambient air. *Inhalation toxicology*, 19(5), 419-449, doi:10.1080/08958370601174941, 2007.
- Savarino, J., Bekki, S., ColeDai, J., & Thiemens, M. H.: Evidence from sulfate mass independent oxygen isotopic compositions of dramatic changes in atmospheric oxidation following massive volcanic eruptions. *Journal of Geophysical Research*, 108(D21), 4671, doi:10.1029/2003JD003737, 2003.
- Savarino, J., Kaiser, J., Morin, S., Sigman, D. M., & Thiemens, M. H.: Nitrogen and oxygen isotopic constraints on the origin of atmospheric nitrate in coastal Antarctica. *Atmospheric Chemistry and Physics*, 7(8), 1925-1945, doi:10.5194/acp-7-1925-2007, 2007.
- Savarino, J., Lee, C. C., & Thiemens, M. H.: Laboratory oxygen isotopic study of sulfur (IV) oxidation: Origin of the mass-independent oxygen isotopic anomaly in atmospheric sulfates and sulfate mineral deposits on Earth. *Journal of Geophysical Research*, 105(D23), 29,079-29,088, doi:10.1029/2000JD900456, 2000.
- Seigneur, C., & Saxena, P.: A theoretical investigation of sulfate formation in clouds. *Atmospheric Environment* (1967), 22(1), 101-115, doi:10.1016/0004-6981(88)90303-4, 1988.



- Smith, S. J., van Aardenne, J., Klimont, Z., Andres, R. J., Volke, A., & Delgado Arias, S.: Anthropogenic sulfur dioxide emissions: 1850-2005. *Atmospheric Chemistry and Physics*, 11(3), 1101-1116, doi:10.5194/acp-11-1101-2011, 2011.
- Sofen, E. D., Alexander, B., & Kunasek, S. A.: The impact of anthropogenic emissions on atmospheric sulfate production pathways, oxidants, and ice core $\Delta^{17}\text{O}(\text{SO}_4^{2-})$. *Atmospheric Chemistry and Physics*, 11(7), 3565-3578, doi:10.5194/acp-11-3565-2011, 2011.
- Vannucci, P. F., Foley, K., Murphy, B. N., Hogrefe, C., Cohen, R. C., & Pye, H. O.: Temperature-Dependent Composition of Summertime PM_{2.5} in Observations and Model Predictions across the Eastern US. *ACS Earth and Space Chemistry*, 8(2), 381-392, doi:10.1021/acsearthspacechem.3c00333, 2024.
- 505 Vicars, W. C., & Savarino, J.: Quantitative constraints on the O-17-excess ($\Delta^{17}\text{O}$) signature of surface ozone: Ambient measurements from 50°N to 50°S using the nitrite-coated filter technique. *Geochimica et Cosmochimica Acta*, 135, 270-287, doi:10.1016/j.gca.2014.03.023, 2014.
- Walters, W. W., Michalski, G., Böhlke, J. K., Alexander, B., Savarino, J., & Thiemens, M. H.: Assessing the seasonal dynamics of nitrate and sulfate aerosols at the South Pole utilizing stable isotopes. *Journal of Geophysical Research: Atmospheres*, 124(14), 8161-8177. doi:10.1029/2019JD030517, 2019.
- 510 Weber, R. J., Guo, H., Russell, A. G., & Nenes, A.: High aerosol acidity despite declining atmospheric sulfate concentrations over the past 15 years. *Nature Geoscience*, 9(4), 282-285, doi:10.1038/ngeo2665, 2016.
- Weston, R. E. Jr.: When is an isotope effect non-mass dependent. *Journal of Nuclear Science and Technology*, 43(4), 295-299, doi:10.1080/18811248.2006.9711092, 2006.
- 515 Yarwood, G., Jung, J., Whitten, G. Z., Heo, G., Mellberg, J., & Estes, M.: Updates to the Carbon Bond mechanism for version 6 (CB6), in : Proceedings the of 9th Annual CMAS Conference, Chapel Hill, NC, October 11-13, 2010, 11-13, 2010.